Supplementary Information

Silk Fibroin-Based Hydrogel Desensitizer Achieving 660 μm Dentin Tubule Occlusion for Dentin Hypersensitivity Treatment

Kuangdi Xin[ab]‡, Wanshan Gao[abcd] ‡, Yulu Xie[a], Xiaohua Dong[a], Lingshan Ran[a], Tianyi Xia[b], Jing Xie[b], Jiaojiao Yang[c], Tao Hu[cd], Jianshu Li[bc], Xiaoyu Huang[e*], Rongmin Qiu[a*], Jun Luo[b*]

Affiliations:
a College of Stomatology, Hospital of Stomatology Guangxi Medical University, Guangxi Key Laboratory of Oral and Maxillofacial Rehabilitation and Reconstruction, Guangxi Clinical Research Center for Craniofacial Deformity, Guangxi Key Laboratory of Oral and Maxillofacial Surgery Disease Treatment, Guangxi Health Commission Key Laboratory of Prevention and Treatment for Oral Infectious Diseases, Nanning 530021, P.R. China.
b College of Polymer Science and Engineering, State Key Laboratory of Advanced Polymer Materials, Sichuan University, Chengdu 610065, P. R. China.
c State Key Laboratory of Oral Diseases, West China Hospital of Stomatology, Sichuan University, Chengdu 610041, P. R. China.
d National Center for Stomatology, National Clinical Research Center for Oral Diseases, Frontier Innovation Center for Dental Medicine Plus, Sichuan University, Chengdu 610041, P. R. China
e Department of Preventive Dentistry, School and Hospital of Stomatology, Fujian Medical University, Fuzhou, Fujian Province, P.R. China.

‡The authors contribute equally to this work.

*: Correspondence author

Correspondence to: Xiaoyu Huang, email: hxy@fjmu.edu.cn; Rongmin Qiu, email: rongminqiu@hotmail.com; Jun Luo, email: luojuncd@scu.edu.cn.

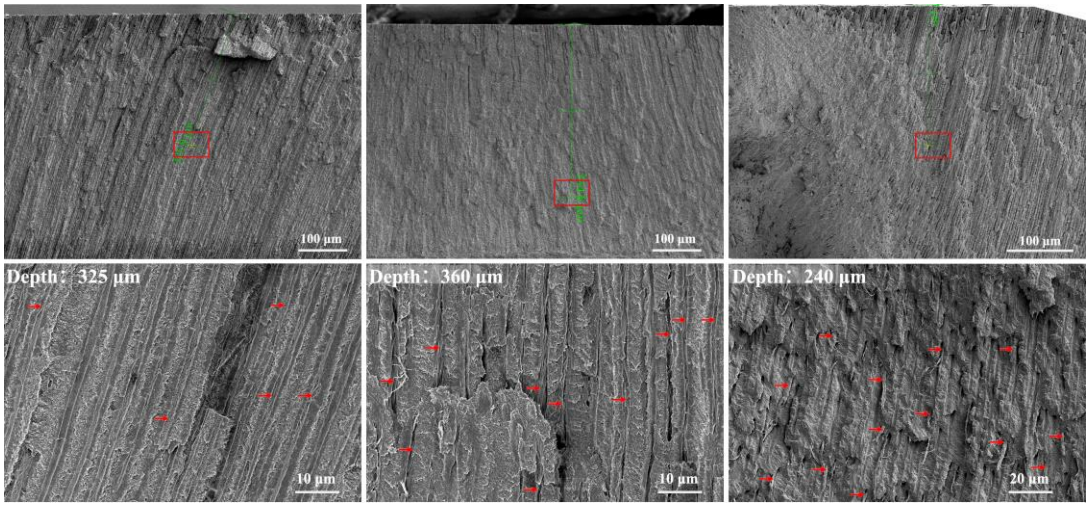

Figure S1. Additional SEM images illustrate the abundant presence of STU within the deeper regions of DTs, extensively forming dense and continuous occlusion.

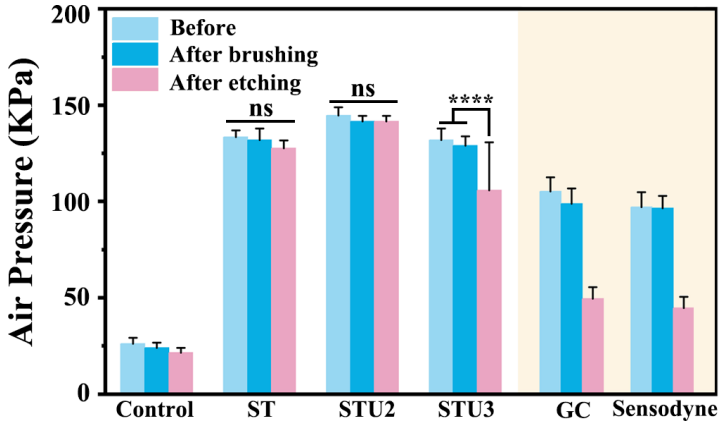

Figure S2. Air pressure profiles of dentin slices treated with ST, STU, and remineralization-based desensitizing agents (GC Tooth Mousse™ and Sensodyne™) before and after brushing and subsequent acid etching, analyzed using one-way ANOVA followed by Tukey's post-hoc test (n = 3, ns = not significant, ****$p < 0.0001$).

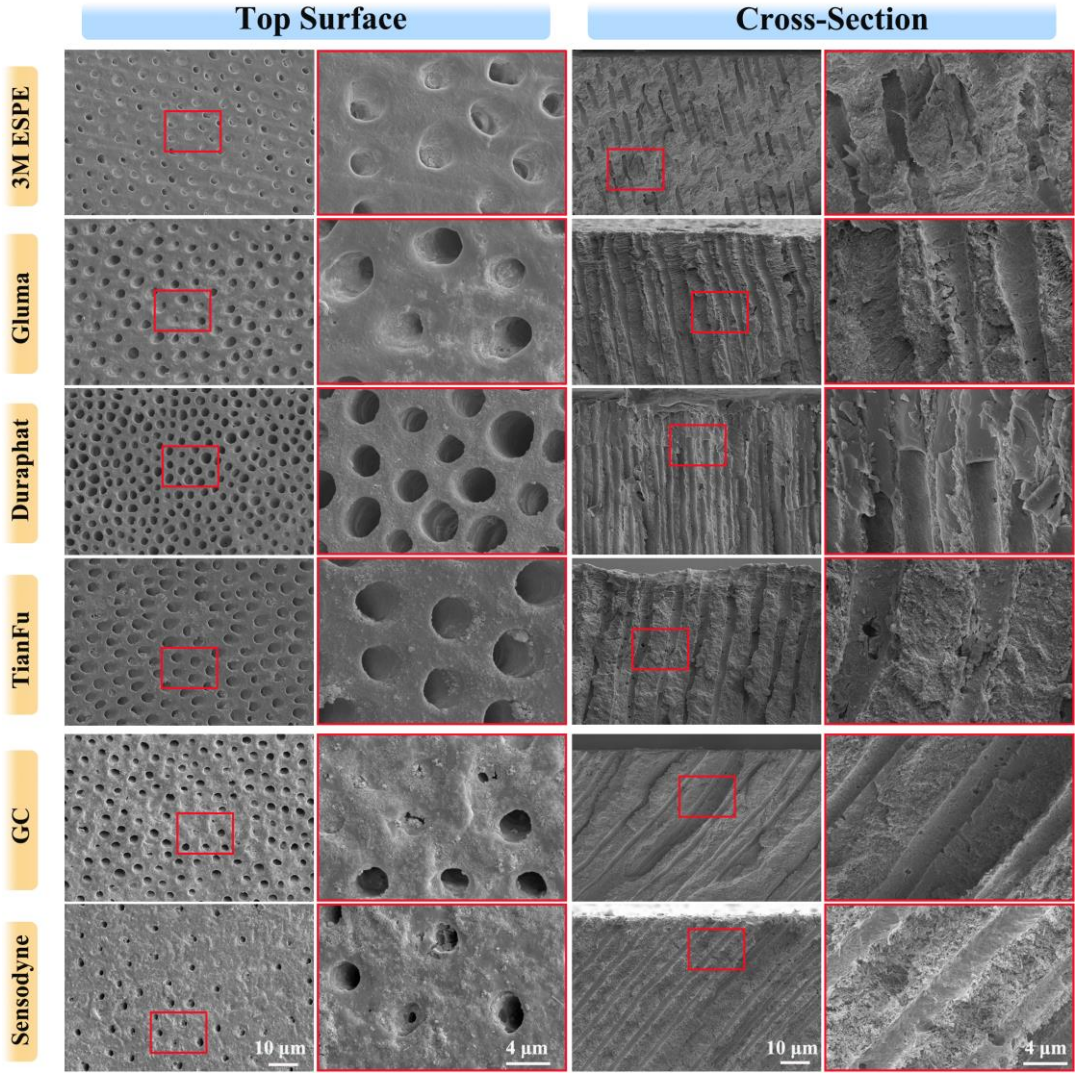

Figure S3. SEM images of the top surface and cross-sections of dentin slices treated with various commercial desensitizing agents. 3M ESPE™, Gluma™, Duraphat™, and Tianfu™ were applied for immediate occlusion, while GC Tooth Mousse™ (containing CPP-ACP) and Sensodyne™ (containing Novamin) were evaluated after 14 d of remineralization. All groups exhibited inadequate deep occlusion of DTs.

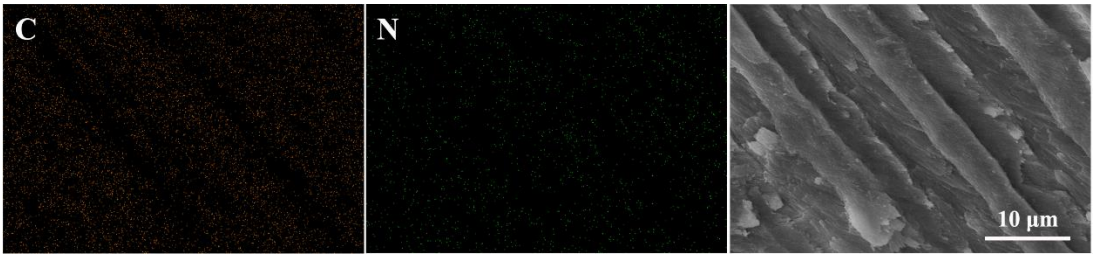

Figure S4. EDS mapping of the SEM image in Figure 4I.

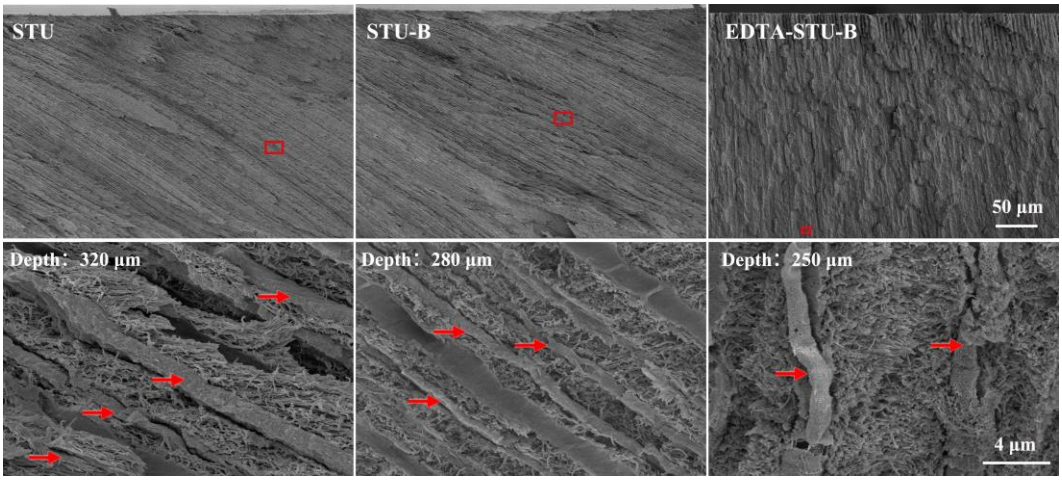

Figure S5. SEM images illustrate the ability of STU to resist external erosion within the deeper regions of DTs under pH cycle, both normal group with demineralize solution and aggressive subgroup with 2%EDTA solution.

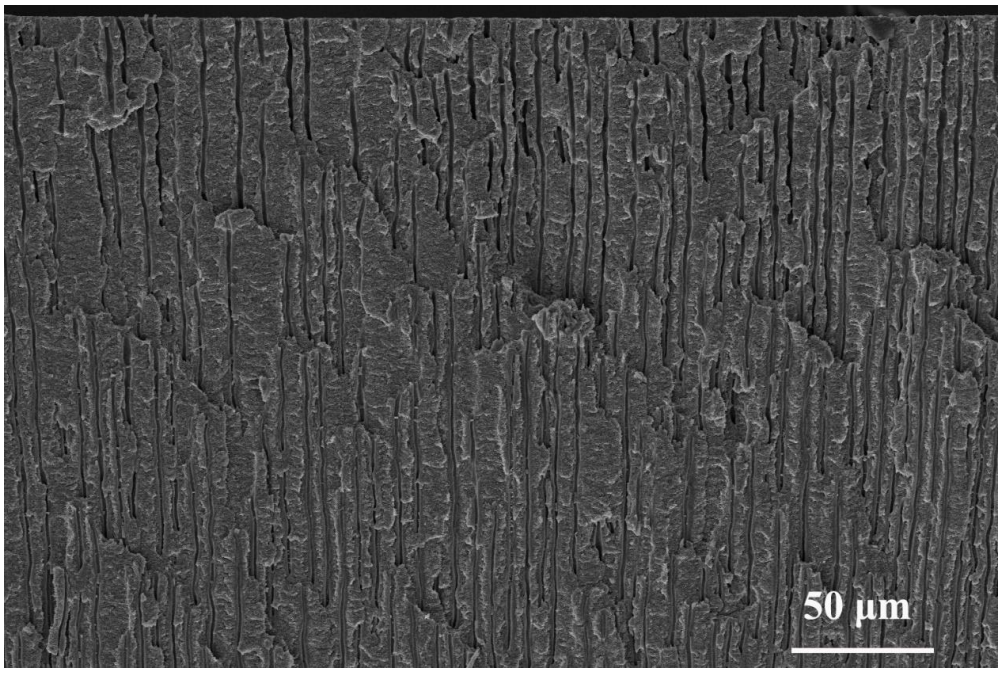

Figure S6. SEM images illustrate the ability of ST hydrogel within DTs to resist external erosion under pH cycle. In this large view, few ST hydrogel could be captured and resulted in a poor occlusion.

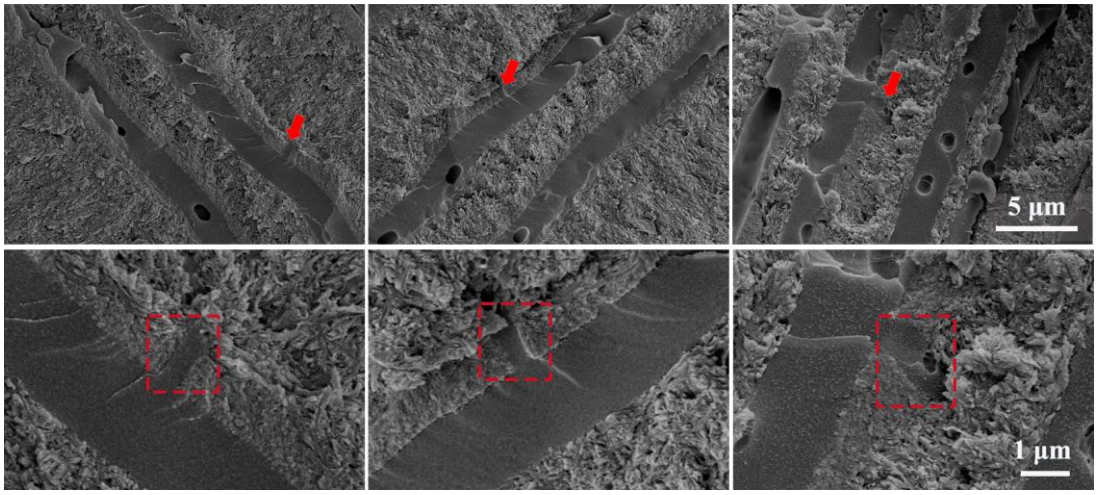

Figure S7. SEM images illustrate the close contact and thorough filling of STU hydrogel within narrow DTs. Enlarged views (bottom row) highlight the intimate adaptation to tubule wall microstructures, supporting enhanced sealing through increased contact area.

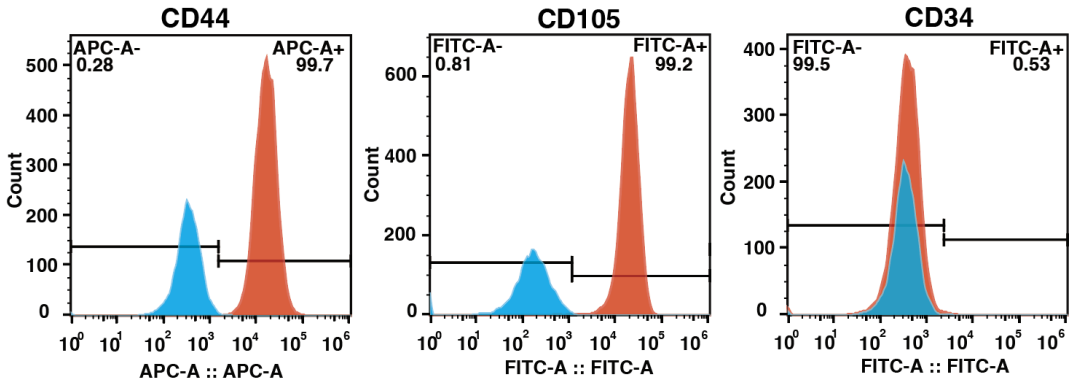

Fig. S8 Flow cytometry was used to analyze the surface markers of HDPSCs; Positive rate: CD44-99.7%, CD105- 99.2%, CD34-0.53%.

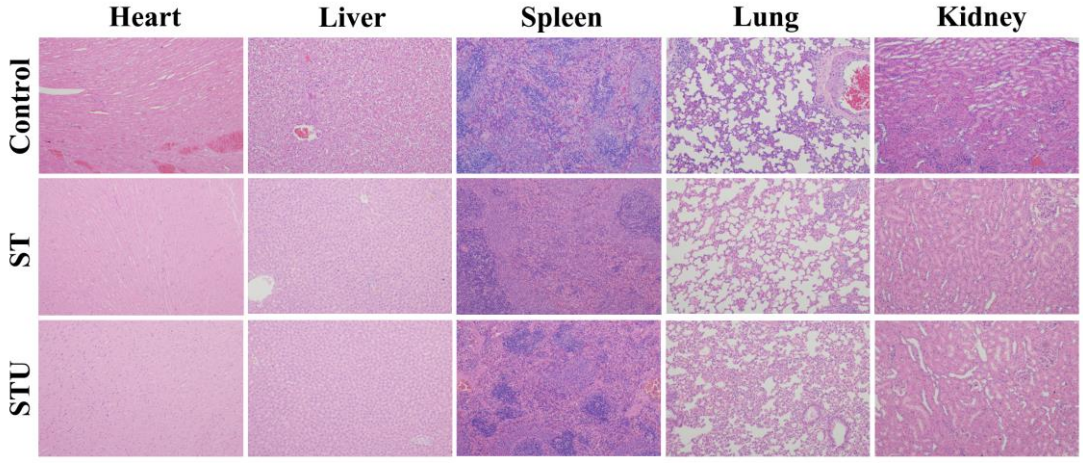

Figure S9. Biocompatibility evaluation of ST hydrogels in rats. Histological section images by H&E staining.

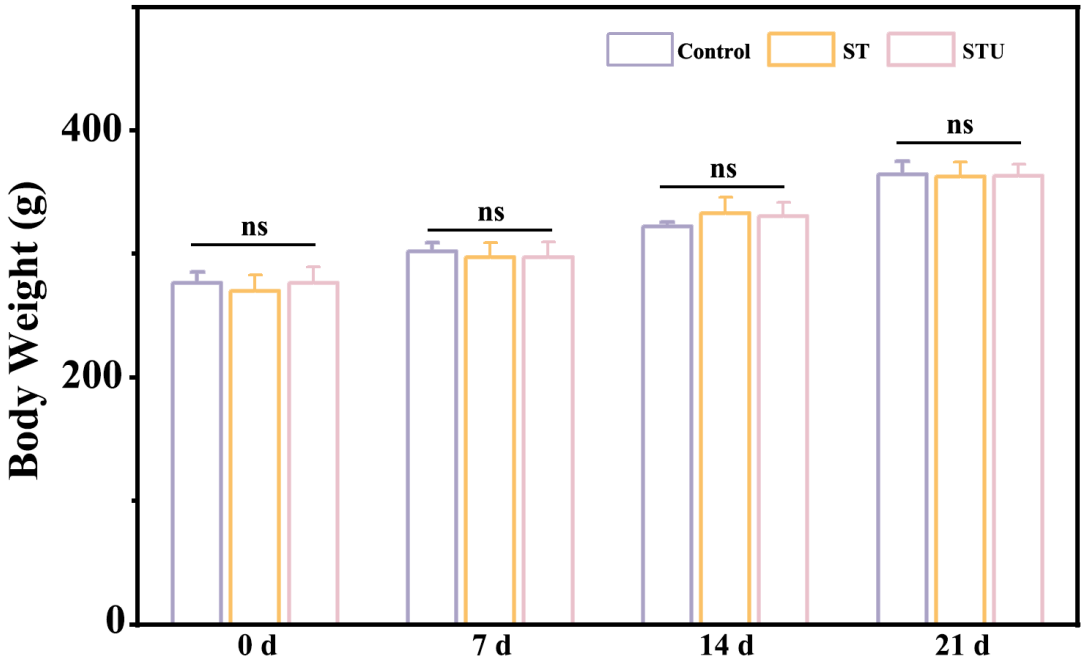

Figure S10. Changes in rats' body weight during the *semi-in vivo* experiment in 21 d. The error bars represent the mean ± SD for n = 3, ns = not significant.

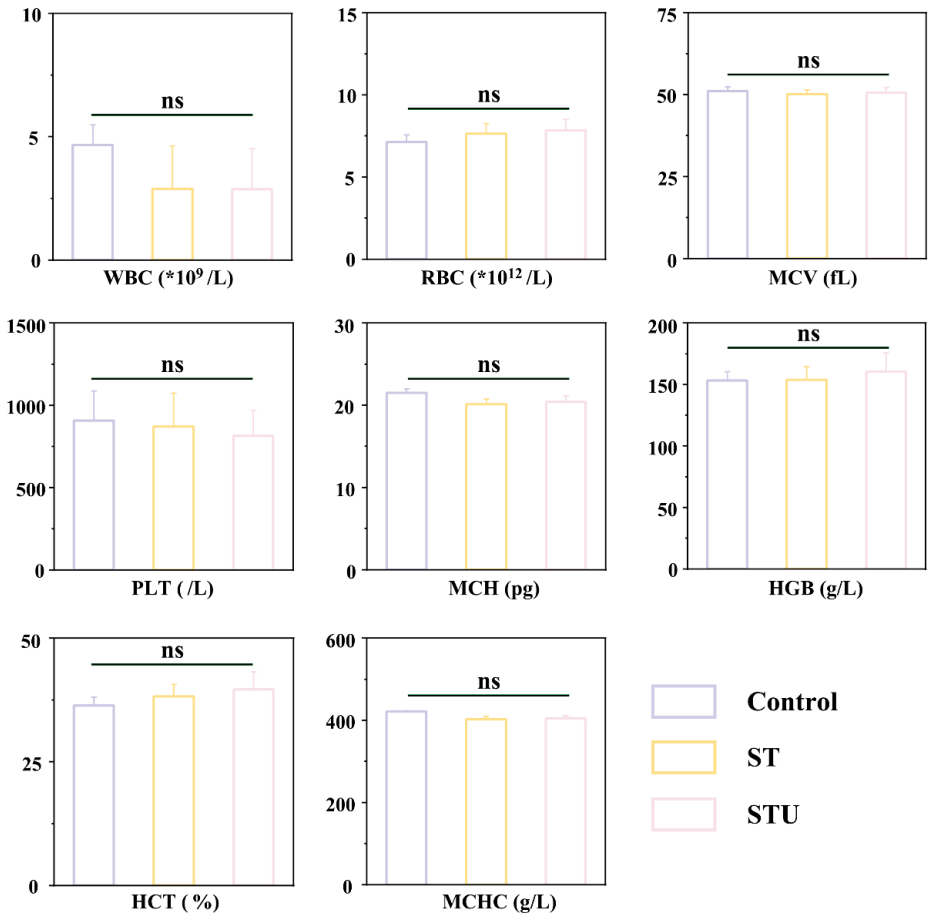

Figure S11. Hematology (WBC, RBC, MCV, PLT, MCH, HGB, HCT, MCHC) of the rats in different groups for 21 d. The error bars represent the mean ± SD for n = 3, ns = not significant.

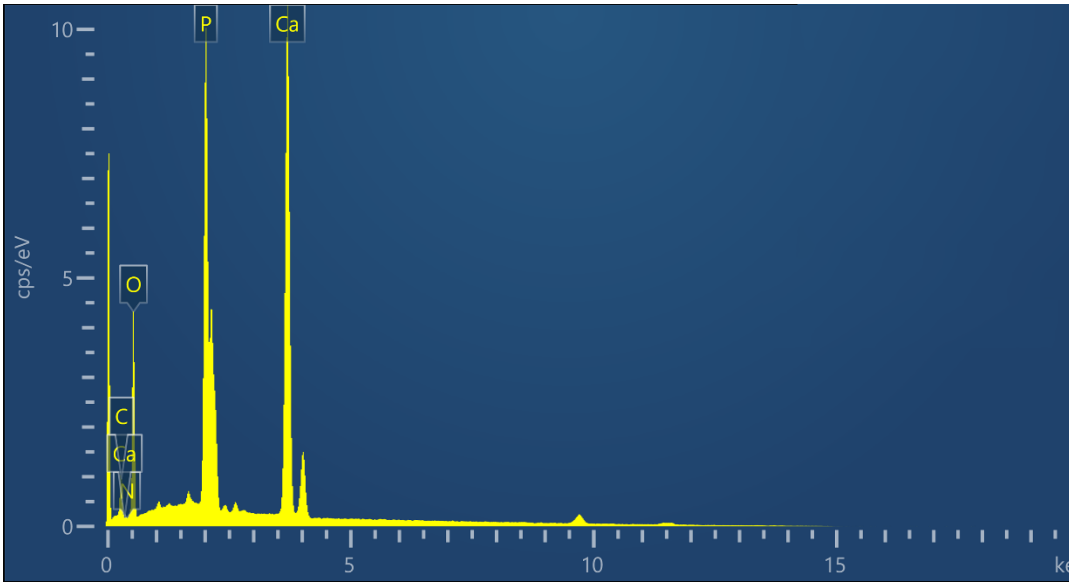

Figure S12. EDS analysis showing the elements of Figure 7 D3.

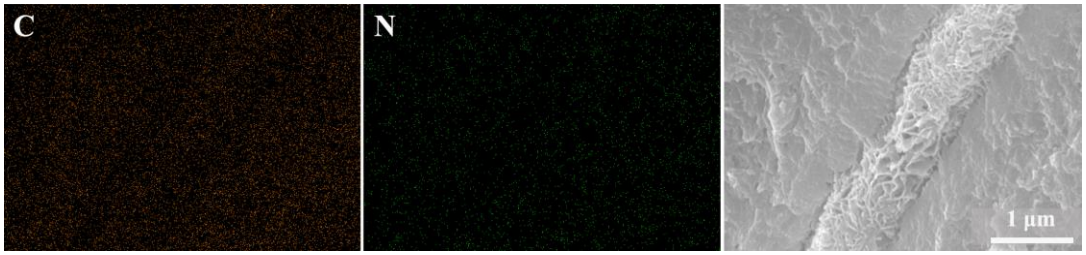

Figure S13. EDS mapping of the SEM image in Figure 8D (Green Border).

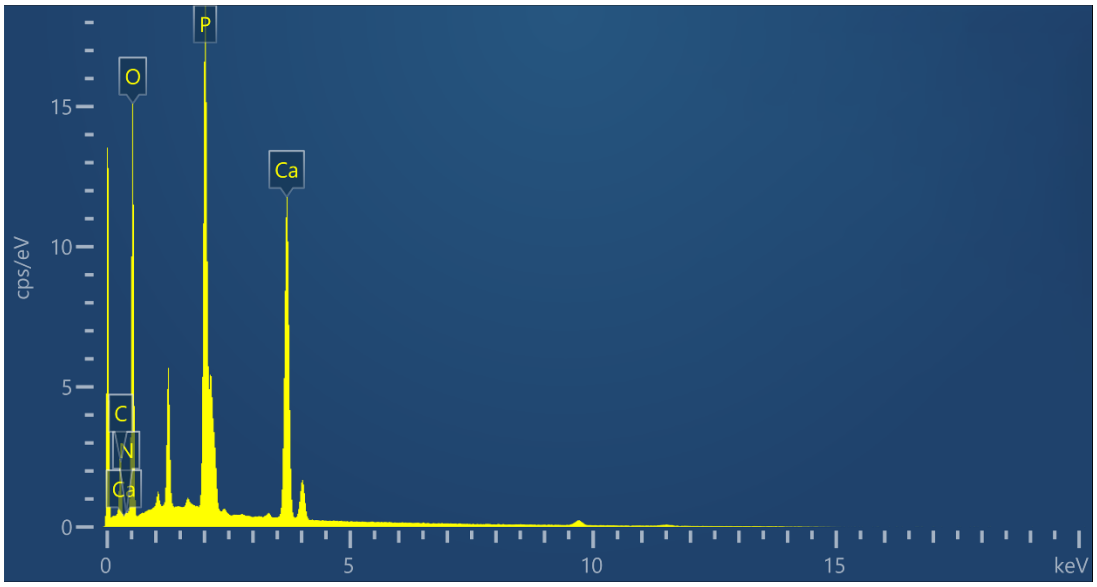

Figure S14. EDS analysis showing the elements of Figure S13.

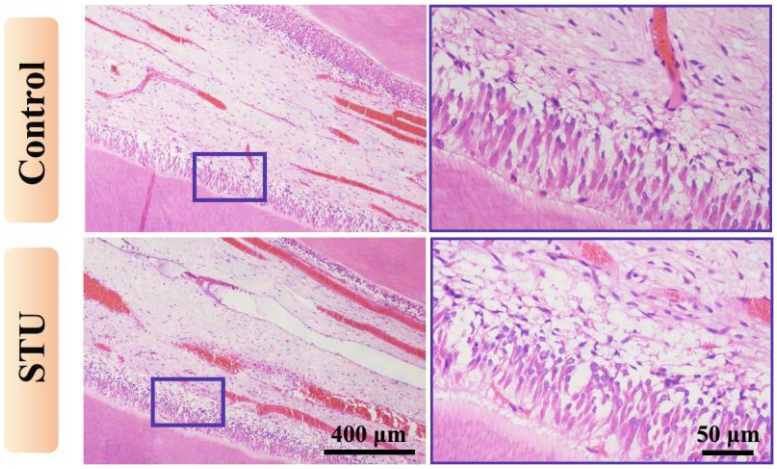

Figure S15. H&E staining of rabbit dental pulp after surface application of STU.

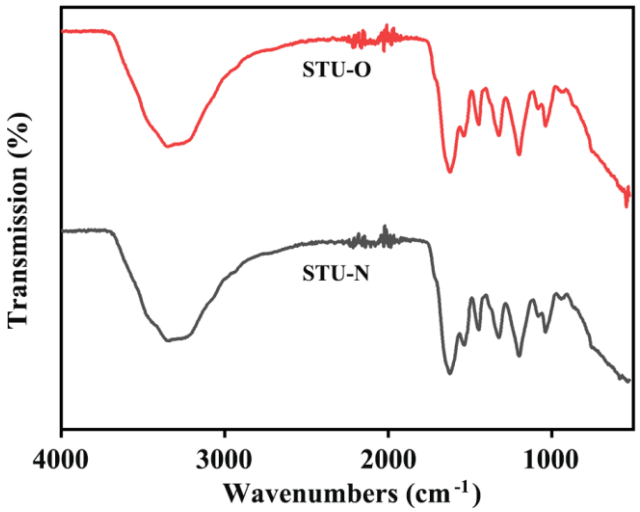

Figure S16. A comparation on FTIR spectra between fresh STU(STU-N) and stored STU which is reconstructed by adding water to a lyophilized powder that has been stored for 10 m (STU-O). The nearly identical characteristic peaks in the FTIR spectra comparison indicate that the STU hydrogel regenerated from the lyophilized powder stored in a sealed condition for approximately 10 m maintains a chemical composition essentially consistent with that of freshly prepared STU. This suggests that the STU lyophilized powder retains the ability to restore into a complete STU hydrogel even after long-term storage under general conditions.

Movie S1. The feasibility of the modified-Transwell dentin device (modified-TDD) was tested. As citric acid gradually permeated through the barrier of control group into the lower chamber, the resulting pH change caused the litmus color to shift from purple (neutral) to red (acidic), making it easy to observe. In contrast, both the blank group and the STU group showed no significant color change during the evaluation, indicating that the modified Transwell chamber membrane in these groups had a good isolation effect.